

DELFT UNIVERSITY OF TECHNOLOGY

REPORT 08-02

ON AN OPTION PRICING METHOD BASED ON FOURIER-COSINE SERIES
EXPANSIONS

F. FANG AND C. W. OOSTERLEE

ISSN 1389-6520

Reports of the Department of Applied Mathematical Analysis

Delft 2008

Copyright © 2008 by Delft Institute of Applied Mathematics Delft, The Netherlands.

No part of the Journal may be reproduced, stored in a retrieval system, or transmitted, in any form or by any means, electronic, mechanical, photocopying, recording, or otherwise, without the prior written permission from Delft Institute of Applied Mathematics, Delft University of Technology, The Netherlands.

A Novel Option Pricing Method based on Fourier-Cosine Series Expansions

Part I: European products

F. Fang*, C.W. Oosterlee†

January 29, 2008

Abstract

Here we develop an option pricing method for European options based on the Fourier-cosine series, and call it the COS method. The convergence rate of the COS method is exponential and the computational complexity is linear. It has a wide range of applicability for different underlying dynamics, including Lévy processes and Heston's stochastic volatility model, and for various types of option contracts. We will present the method and its applications in two separate parts. The first one is this paper, where we deal in particular with European options. In a follow-up paper, part II, we will present its application to options with early-exercise features.

1 Introduction

Efficient numerical methods are required to rapidly price complex contracts and calibrate various financial models.

In option pricing, it is the famous Feynman-Kac theorem that relates the conditional expectation of the value of a contract payoff function under the risk-neutral measure to the solution of a partial differential equation. In the research areas covered by this theorem, various numerical pricing techniques can be developed. Briefly speaking, existing numerical methods can be classified into three major groups: partial-(integro) differential equation (PIDE) methods, monte Carlo simulation and numerical integration methods. Each of them has its merits and demerits for specific applications in finance, but the methods from the latter class are often used for calibration purposes. An important aspect of research in computational finance is to further increase the performance of the pricing methods.

*Delft University of Technology, Delft Institute of Applied Mathematics, Delft, the Netherlands, email: f.fang@ewi.tudelft.nl

†CWI – Centrum Wiskunde & Informatica, Amsterdam, the Netherlands, email: c.w.oosterlee@cwi.nl, and Delft University of Technology, Delft Institute of Applied Mathematics.

State-of-the-art numerical integration techniques have in common that they rely on a transformation to the Fourier domain [7, 18]. The Carr-Madan method [7] is one of the best known examples of this class. The probability density function appears in the integration, which is not known for many relevant pricing processes. However, its Fourier transform, the characteristic function, is often available, for example, from the Lévy-Khinchine theorem for underlying Lévy processes or by other means, as for Heston’s model. In the Fourier domain it is possible to solve various derivative contracts, as long as the characteristic function is available. By means of the Fast Fourier Transform (FFT) integration can be performed with a computational complexity of $O(N \log_2 N)$, where N represents the number of integration points. The computational speed, especially for plain vanilla options, makes the integration methods state-of-the-art for calibration at financial institutions.

Quadrature rule based techniques are, however, not of the highest efficiency when solving Fourier transformed integrals. Due to the fact that the integrands are highly oscillatory, a relatively fine grid has to be used for satisfactory accuracy with the FFT.

In this paper we will focus on *Fourier-cosine expansions* in the context of numerical integration, as an alternative for the methods based on the FFT. We will show that this novel method, called the COS method, can further improve the speed of pricing plain vanilla and some exotic options. Its application to American style products will be covered in a follow-up paper. It is due to the impressive speed reported here that we devote a paper to the European style products.

This paper is organized as follows. In Section 2, we introduce the Fourier cosine expansion for solving inverse Fourier integrals. Based on this, we derive, in Section 3, the formulas for pricing European options and the Greeks. We focus on the Lévy and Heston price processes for the underlying. An error analysis is presented in Section 4 and numerical results are given in Section 5.

2 Fourier Integrals and Cosine Series

The point-of-departure for pricing European options with numerical integration techniques is the risk-neutral valuation formula:

$$v(t_0, x) = e^{-r\Delta t} \mathbb{E}^{\mathbb{Q}} [v(T, y)] = e^{-r\Delta t} \int_{\mathbb{R}} v(T, y) f_{Y|X}(y|x) dy, \quad (1)$$

where v denotes option value, Δt is the difference between the maturity, T , and the initial date, t_0 , and $\mathbb{E}^{\mathbb{Q}}[\cdot]$ is the expectation operator under risk-neutral measure \mathbb{Q} . x and y are state variables at time t_0 and T , respectively; $f_{Y|X}(y|x)$ is the probability density of y given x and r is the risk-neutral interest rate.

In the state-of-the-art Carr-Madan approach [7] the Fourier transform of a version of valuation formula (1) is taken with respect to the log-strike price. Damping of the payoff is then necessary as, for example, a call option is not L^1 -integrable with respect to the logarithm of the strike price. The method’s accuracy depends on the correct value of the damping parameter. A closed-form expression for the resulting integral is available in

Fourier space. To return to the time domain, quadrature rules have to be applied to the inverse Fourier integral for which the application of the FFT algorithm is appropriate.

The range of applicability of numerical integration methods in finance has recently been increased by the presentation of efficient techniques for options with early exercise features [7, 18, 2, 3, 17]. Especially the CONV method [17] achieves almost linear complexity, also with the help of the FFT algorithm, for Bermudan and American options. This method can also be efficiently used for European options and numerical experiments in [17] show that the accuracy is not influenced by the choice of the damping parameter. The difference with the Carr-Madan approach is that the transform is taken with respect to the log-spot price in the CONV method instead of the log-strike price (something which [16] and [20] also consider). In the derivation of the CONV method the risk-neutral valuation formula is rewritten as a cross-correlation between the option value and the transition density. The cross-correlation is handled numerically by replacing the option value by its Fourier-series expansion so that the cross-correlation is transformed to an inner product of series coefficients. The coefficients are recovered by applying quadrature rules, combined with the FFT algorithm. Error analysis and experimental results have demonstrated second order accuracy and $O(N \log(N))$ computational complexity for European options.

These numerical integration methods have to numerically solve the forward or the inverse¹ Fourier integrals:

$$\phi(\omega) = \int_{\mathbb{R}} e^{ix\omega} f(x) dx \quad (2)$$

$$f(x) = \frac{1}{2\pi} \int_{\mathbb{R}} e^{-i\omega x} \phi(\omega) d\omega. \quad (3)$$

The density and its characteristic function are an example of a Fourier pair. Existing numerical integration methods in finance typically compute Fourier integrals by applying equally spaced numerical integration rules on the integrals then employing the FFT algorithm by imposing the Nyquist relation to the grid sizes in the x - and ω -domains,

$$\Delta x \cdot \Delta \omega \equiv 2\pi/N,$$

with N the number of grid points. The grid values can then be obtained in $O(N \log_2 N)$ operations. However, there are three disadvantages: The error convergence of equally spaced integration rules, except the Clenshaw-Curtis rule, is not very high; N has to be a power of two; and, finally, the relation imposed on the grid sizes prevents one from using fine grids in both domains.

Remark 2.1. *In principle we could use the Fractional FFT algorithm (FrFT) which does not require the Nyquist relation to be satisfied, as in [8]. Numerical tests indicated however that this advantage of the FrFT did not outweigh the speed of the FFT.*

¹Here we use the convention of the Fourier transform definition often seen in the financial engineering literature. Other conventions can also be used and modifications to the methods are then straightforward.

Remark 2.2. *Alternative methods for the forward Fourier integral, based on replacing $f(x)$ in (2) by its Chebyshev [19] or Legendre [12] polynomial expansion, can achieve a high accuracy with only a limited number of terms in the expansion. However, the resulting computational complexity is typically at least quadratic.*

2.1 Inverse Fourier Integral via Cosine Expansion

In this section, as a first step, we present a different methodology for solving, in particular, the inverse Fourier integral in (3). The main idea is to reconstruct the whole integral – not just the integrand – from its Fourier-cosine series expansion (also called ‘cosine expansion’), extracting the series coefficients directly from the integrand. Fourier-cosine series expansions usually give an optimal approximation of functions with a finite support² [5]. In fact, the cosine expansion of $f(x)$ in x equals the Chebyshev series expansion of $f(\cos^{-1}(t))$ in t .

For a function supported on $[0, \pi]$, the cosine expansion reads

$$f(\theta) = \sum_{k=0}^{\prime\infty} A_k \cdot \cos(k\theta) \quad \text{with} \quad A_k = \frac{2}{\pi} \int_0^\pi f(\theta) \cdot \cos(k\theta) d\theta, \quad (4)$$

where \sum' indicates that the first term in the summation is weighted by one-half. For functions supported on any other finite interval, say $[a, b] \in \mathbb{R}$, the Fourier-cosine series expansion can easily be obtained via a change of variables,

$$\theta := \frac{x-a}{b-a}\pi; \quad x = \frac{b-a}{\pi}\theta + a.$$

It then reads

$$f(x) = \sum_{k=0}^{\prime\infty} A_k \cdot \cos\left(k \cdot \frac{x-a}{b-a}\pi\right), \quad (5)$$

with

$$A_k = \frac{2}{b-a} \int_a^b f(x) \cdot \cos\left(k \cdot \frac{x-a}{b-a}\pi\right) dx. \quad (6)$$

Since any real function has a cosine expansion when it is finitely supported, the derivation starts with a truncation of the infinite integration range in (3). Due to the conditions for the existence of a Fourier transform, the integrands in (3) have to decay to zero at $\pm\infty$ and we can truncate the integration range in a proper way without losing accuracy.

Suppose $[a, b] \in \mathbb{R}$ is chosen such that the truncated integral approximates the infinite counterpart very well, i.e.,

$$\phi_1(\omega) := \int_a^b e^{i\omega x} f(x) dx \approx \int_{\mathbb{R}} e^{i\omega x} f(x) dx = \phi(\omega), \quad (7)$$

By subscripts for variables, like i in ϕ_i , we denote subsequent numerical approximations (not to be confused with subscripted series coefficients, A_k and F_k).

²The usual Fourier series expansion is actually superior when a function is periodic.

Comparing equation (7) with the cosine series coefficients of $f(x)$ on $[a, b]$ in (6), we find that

$$A_k \equiv \frac{2\text{Re} \left\{ \phi_1 \left(\frac{k\pi}{b-a} \right) \cdot \exp \left(-i \frac{ka\pi}{b-a} \right) \right\}}{b-a}, \quad (8)$$

where $\text{Re} \{ \cdot \}$ denotes taking the real part of the argument. It then follows from (7) that $A_k \approx F_k$, with

$$F_k \equiv \frac{2\text{Re} \left\{ \phi \left(\frac{k\pi}{b-a} \right) \cdot \exp \left(-i \frac{ka\pi}{b-a} \right) \right\}}{b-a}.$$

We now replace A_k by F_k in the series expansion of $f(x)$ on $[a, b]$, i.e.

$$f_1(x) \approx \sum_{k=0}^{\infty} F_k \cos \left(k\pi \frac{x-a}{b-a} \right), \quad (9)$$

and truncate the series summation such that

$$f_2(x) \approx \sum_{k=0}^{N-1} F_k \cos \left(k\pi \frac{x-a}{b-a} \right). \quad (10)$$

The resulting error in $f_2(x)$ consists of two parts: a series truncation error from (9) to (10) and an error originating from the approximation of A_k by F_k . An error analysis that takes these different approximations into account is presented in Section 4.

Since the cosine series expansion of *entire functions* (i.e., functions without any singularities³ anywhere in the complex plane, except at ∞) exhibits an *exponential convergence* [5], we can expect (10) to give highly accurate approximations to functions that have no singularities on $[a, b]$, with a small N .

To demonstrate this, we evaluate here equation (10), where

$$f(x) = \frac{1}{\sqrt{2\pi}} e^{-\frac{1}{2}x^2},$$

and determine the accuracy for different values of N . We choose $[a, b] = [-10, 10]$ and the maximum error is measured at $x = \{-5, -4, \dots, 4, 5\}$.

Table 1 indicates that a very small error is obtained with a only small number of terms, N , in the expansion.

Table 1: Maximum error when recovering $f(x)$ from $\phi(\omega)$ by Fourier cosine expansion.

N	4	8	16	32	64
error	0.0499	0.0248	0.0014	3.50e-08	8.33e-17
cpu time (msec.)	0.0025	0.0028	0.0025	0.0031	0.0032

This technique is found to be highly efficient for the recovery of the density function, as will be presented in Section 5.

³By ‘singularity’ we mean [5] poles, fractional powers, logarithms, other branch points and discontinuities in a function or in any of its derivatives.

3 Pricing European Options

In this section, we derive the COS formula for European style options by replacing the density function by its Fourier cosine series. We make use of the fact that a density function tends to be smooth and therefore only a few terms in the expansion may already give a good approximation.

Since the density rapidly decays to zero as $y \rightarrow \pm\infty$ in (1), we truncate the infinite integration range without losing significant accuracy to $[a, b] \subset \mathbb{R}$, and obtain approximation v_1 :

$$v_1(t_0, x) = e^{-r\Delta t} \int_a^b v(T, y) f_{Y|X}(y|x) dy. \quad (11)$$

An area, $[a, b]$, which covers $[x - 10\sigma, x + 10\sigma]$ is often sufficiently accurate, with σ the standard deviation of the density. In the case of fat tailed distributions, which we also consider in this paper, we need larger domains.

In the second step, since $f_{Y|X}(y|x)$ is usually not known whereas the characteristic function is, we replace the density by its cosine expansion in y ,

$$f_{Y|X}(y|x) = \sum_{k=0}^{+\infty} A_k(x) \cos\left(k\pi \frac{y-a}{b-a}\right) \quad (12)$$

with

$$A_k(x) := \frac{2}{b-a} \int_a^b f_{Y|X}(y|x) \cos\left(k\pi \frac{y-a}{b-a}\right) dy. \quad (13)$$

So,

$$v_1(t_0, x) = e^{-r\Delta t} \int_a^b v(T, y) \sum_{k=0}^{+\infty} A_k(x) \cos\left(k\pi \frac{y-a}{b-a}\right) dy. \quad (14)$$

We interchange the summation and integration,

$$v_1(t_0, x) = e^{-r\Delta t} \sum_{k=0}^{+\infty} A_k(x) \cdot V_k \quad (15)$$

with

$$V_k := \int_a^b v(T, y) \cos\left(k\pi \frac{y-a}{b-a}\right) dy, \quad (16)$$

which is a scaled cosine series coefficient of $v(T, y)$ in y . Thus, from (11) to (15) we have transformed the inner product of two real functions, $f_{Y|X}(y|x)$ and $v(T, y)$, to that of their Fourier-cosine series coefficients.

Due to the rapid decay rate of these coefficients, we further truncate the series summation, resulting in approximation v_2 ,

$$v_2(t_0, x) = e^{-r\Delta t} \sum_{k=0}^{N-1} A_k(x) \cdot V_k. \quad (17)$$

Similarly as in Section 2, coefficients $A_k(x)$ defined in (13) can be approximated by $F_k(x)$, defined as

$$F_k(x) := 2 \frac{\operatorname{Re} \left\{ \phi \left(\frac{k\pi}{b-a}; x \right) \exp \left(-i \frac{ka\pi}{b-a} \right) \right\}}{(b-a)} \quad (18)$$

with $\phi(\omega; x)$, the characteristic function, defined by

$$\phi(\omega; x) := \int_{\mathbb{R}} e^{i\omega y} f_{Y|X}(y|x) dy.$$

Replacing $A_k(x)$ by $F_k(x)$ in (17), we finally obtain

$$v_3(t_0, x) = e^{-r\Delta t} \frac{2}{b-a} \sum_{k=0}^{N-1} \operatorname{Re} \left\{ \phi \left(\frac{k\pi}{b-a}; x \right) e^{-ik\pi \frac{a}{b-a}} \right\} \cdot V_k. \quad (19)$$

This is the COS formula for pricing European style options.

We will show next that V_k , the series coefficients of the payoff, can be obtained analytically for vanilla and digital options.

3.1 Coefficients V_k for Plain Vanilla Options

Before we can use (19) for pricing options, the payoff series coefficients, V_k , have to be recovered. We can, however, find analytic solutions for V_k for several contracts.

As we assume here that the characteristic function of the log-asset price is known, we represent the payoff as a function of the log-asset price. Let us denote the log-asset prices by

$$x := \ln(S_0/K) \quad \text{and} \quad y := \ln(S_T/K),$$

with S_t denoting the underlying price at time t and K the strike price. The payoff functions for European options, in log-asset prices, read

$$v(y, T) \equiv [\alpha \cdot K \cdot (e^y - 1)]^+ \quad \text{with} \quad \alpha = \begin{cases} 1 & \text{for call,} \\ -1 & \text{for put.} \end{cases}$$

Before deriving V_k from its definition in (16), we need two mathematical entities.

Definition 3.1. *The cosine series coefficients, χ_k , of $g(y) = e^y$ on $[c, d] \subset [a, b]$,*

$$\chi_k(c, d) := \int_c^d e^y \cos \left(k\pi \frac{d-a}{b-a} \right) dy, \quad (20)$$

and the cosine series coefficients, ψ_k , of $g(y) = 1$ on $[c, d] \subset [a, b]$,

$$\psi_k(c, d) := \int_c^d \cos \left(k\pi \frac{d-a}{b-a} \right) dy. \quad (21)$$

are known analytically.

Basic calculus shows

$$\begin{aligned} \chi_k(c, d) := & \frac{1}{1 + \left(\frac{k\pi}{b-a}\right)^2} \left[\cos\left(k\pi \frac{d-a}{b-a}\right) e^d - \cos\left(k\pi \frac{c-a}{b-a}\right) e^c \right. \\ & \left. + \frac{k\pi}{b-a} \sin\left(k\pi \frac{d-a}{b-a}\right) e^d - \frac{k\pi}{b-a} \sin\left(k\pi \frac{c-a}{b-a}\right) e^c \right], \end{aligned} \quad (22)$$

and

$$\psi_k(c, d) := \begin{cases} \left[\sin\left(k\pi \frac{d-a}{b-a}\right) - \sin\left(k\pi \frac{c-a}{b-a}\right) \right] \frac{b-a}{k\pi} & k \neq 0, \\ (d-c) & k = 0. \end{cases} \quad (23)$$

Focusing, for example, on a call option, we obtain

$$V_k^{call} = \int_0^b K(e^y - 1) \cos\left(k\pi \frac{y-a}{b-a}\right) dy = K(\chi_k(0, b) - \psi_k(0, b)), \quad (24)$$

where χ_k and ψ_k are given by (22) and (23), respectively. Similarly, for a vanilla put, we find

$$V_k^{put} = K(-\chi_k(a, 0) + \psi_k(a, 0)).$$

Analytic expressions can also be obtained for some exotic options.

3.2 Digital and European Barrier Options

Whereas for European products equation (19) always applies, the coefficients V_k are different for different payoff functions. With analytical expressions for these coefficients, the convergence of the COS does not depend on the continuity of the payoff. For those contracts for which the V_k can only be obtained numerically, the error convergence is dominated by the numerical rules employed to determine them.

Digital options are popular in the financial markets for hedging and speculation. They are also important to financial engineers as building blocks for constructing more complex option products. Here, we consider the payoff of a cash-or-nothing call option, as an example, which is 0 if $S_T \leq K$ and K if $S_T > K$. For this contract the ‘cash-or-nothing call’ coefficients, V_k^{conc} , can be obtained analytically:

$$V_k^{conc} = K \int_0^b \cos\left(k\pi \frac{y-a}{b-a}\right) dy = K\psi_k(0, b).$$

We also give the formula for a so-called gap option [13] of a call options whose payoff reads

$$v(T, y) = [K \cdot (e^y - 1) - Rb] \cdot \mathbf{1}_{\{S_T < H\}} + Rb,$$

where $\mathbf{1}_\Psi = 0$ if Ψ is empty and Rb is a so-called rebate, which is paid if the barrier is hit. The time-dependent version of this payoff represents a barrier option. This will be

discussed in part II of this paper. The integral that defines V_k^{gap} for such payoff functions of a call can be split into two parts:

$$V_k^{gap} = \int_0^h K(e^y - 1) \cos\left(k\pi \frac{y-a}{b-a}\right) dy + \int_h^b Rb \cdot \cos\left(k\pi \frac{y-a}{b-a}\right) dy,$$

where $h := \ln(H/K)$. It then follows that

$$V_k^{gap} = K \cdot (\chi_k(0, h) - \psi_k(0, h)) + Rb \cdot \psi_k(h, b). \quad (25)$$

3.3 Lévy Processes and Heston's Model

Pricing formula (19) can be used for European options under any underlying process as long as the characteristic function is known. This is the case for exponential Lévy models and models from the class of regular affine processes of [11], including the exponentially affine jump-diffusion class of [10]. It is worth mentioning that (19) simplifies for the Lévy and Heston model.

Here, we focus on the characteristic function for the different models and refer the reader to the literature, [9, 6, 14] for example, for background information on these processes.

For Lévy processes, whose characteristic functions can be represented by

$$\phi(\omega; x) = \varphi_{levy}(\omega) \cdot e^{i\omega x} \quad \text{with} \quad \varphi_{levy}(\omega) := \phi(\omega; 0), \quad (26)$$

the pricing formula simplifies to

$$v_3(t_0, x) = e^{-r\Delta t} \frac{2}{b-a} \sum_{k=0}^{N-1} \text{Re} \left\{ \varphi_{levy} \left(\frac{k\pi}{b-a} \right) e^{ik\pi \frac{x-a}{b-a}} \right\} V_k. \quad (27)$$

In particular, for the CGMY/KoBoI model, which encompasses the Geometric Brownian Motion (GBM) and Variance Gamma (VG) models, the characteristic function of the log-asset price is of the form:

$$\begin{aligned} \varphi_{levy}(\omega) &= \exp(i\omega(r-q)\Delta t - \frac{1}{2}\omega^2\sigma^2\Delta t) \cdot \\ &\quad \exp(\Delta t C \Gamma(-Y)[(M-i\omega)^Y - M^Y + (G+i\omega)^Y - G^Y]), \end{aligned} \quad (28)$$

where q is a continuous dividend yield, $\Gamma(\cdot)$ represents the gamma function. In the CGMY model, the parameters should satisfy $C \geq 0, G \geq 0, M \geq 0$ and $Y < 2$. When $\sigma = 0$ and $Y = 0$ we obtain the Variance Gamma (VG) model; for $C = 0$ the Black-Scholes model is obtained.

Remark 3.1. *Note that, (27) is an expression with independent variable x . It is therefore possible to obtain the option prices on different strikes in one single numerical experiment, by choosing a K -vector as the input x -vector.*

In Heston's model the volatility, denoted by \sqrt{u} , is modeled by a stochastic differential equation,

$$\begin{aligned} dx_t &= \left(\mu - \frac{1}{2}u_t\right) dt + \sqrt{u_t}dW_{1t}, \\ du_t &= -\lambda(u_t - \bar{u})dt + \eta\sqrt{u_t}dW_{2t} \end{aligned} \quad (29)$$

where x_t denotes the log-asset price variable and u_t the volatility of the asset price process. Parameters $\lambda \geq 0, \bar{u} \geq 0$ and $\eta \geq 0$ are called the speed of mean reversion, the mean level of variance and the volatility of volatility, respectively. Furthermore, the Brownian motions W_{1t} and W_{2t} are assumed to be correlated with correlation coefficient ρ .

For Heston's model the COS pricing equation also simplifies, since

$$\phi(\omega; x, u_0) = \varphi_{hes}(\omega; u_0) \cdot e^{i\omega x}, \quad (30)$$

with u_0 the volatility of the underlying asset price at the initial time and $\varphi_{hes}(\omega; u_0) := \phi(\omega; 0, u_0)$. We then find

$$v(t_0, x, u_0) \approx e^{-r\Delta t} \frac{2}{b-a} \sum_{k=0}^{N-1} \text{Re} \left\{ \varphi_{hes} \left(\frac{k\pi}{b-a}; u_0 \right) e^{ik\pi \frac{x-a}{b-a}} \right\} V_k. \quad (31)$$

The characteristic function of the log-asset price, $\varphi_{hes}(\omega; u_0)$, reads

$$\begin{aligned} \varphi_{hes}(\omega; u_0) &= \exp \left(i\omega\mu\Delta t + \frac{u_0}{\eta^2} \left(\frac{1 - e^{-D\Delta t}}{2 - Ge^{-D\Delta t}} \right) (\lambda - i\rho\eta\omega - D) \right) \cdot \\ &\quad \exp \left(\frac{\lambda\bar{v}}{\eta^2} \left(\Delta t(\lambda - i\rho\eta\omega - D) - 2 \log \left(\frac{1 - Ge^{-D\Delta t}}{1 - G} \right) \right) \right), \end{aligned}$$

with

$$D = \sqrt{(\lambda - i\rho\eta\omega)^2 + (\omega^2 + i\omega)\eta^2} \quad \text{and} \quad G = \frac{\lambda - i\rho\eta\omega - D}{\lambda - i\rho\eta\omega + D}.$$

Implementation of the COS formula is straightforward. A Matlab code for it, including the Lévy and Heston models is given in Appendix A.

Remark 3.2 (The Greeks). *Series expansions for the Greeks, e.g. Δ and Γ , can be derived similarly. Since*

$$\Delta = \frac{\partial v}{\partial S_0} = \frac{\partial v}{\partial x} \frac{\partial x}{\partial S_0} = \frac{\partial v}{\partial x} \cdot \frac{1}{S_0}, \quad \Gamma = \frac{\partial^2 v}{\partial S_0^2} = \frac{1}{S_0^2} \left(-\frac{\partial v}{\partial S_0} + \frac{\partial^2 v}{\partial S_0^2} \right),$$

it then follows, for example for Heston's model, from (31) that

$$\Delta \approx e^{-r\Delta t} \frac{2}{b-a} \sum_{k=0}^{N-1} \text{Re} \left\{ \varphi \left(\frac{k\pi}{b-a}; u_0 \right) e^{ik\pi \frac{x-a}{b-a}} \frac{ik\pi}{b-a} \right\} \frac{V_k}{S_0} \quad (32)$$

and

$$\Gamma \approx \frac{2e^{-r\Delta t}}{b-a} \sum_{k=0}^{N-1} \text{Re} \left\{ \varphi \left(\frac{k\pi}{b-a}; u_0 \right) e^{ik\pi \frac{x-a}{b-a}} \left[-\frac{ik\pi}{b-a} + \left(\frac{ik\pi}{b-a} \right)^2 \right] \right\} \frac{V_k}{S_0^2}. \quad (33)$$

It is also easy to obtain the formula for Vega, $\frac{\partial v}{\partial u_0}$, as u_0 only appears in the coefficients:

$$\frac{\partial v(t_0, x, u_0)}{\partial u_0} \approx e^{-r\Delta t} \frac{2}{b-a} \sum_{k=0}^{N-1} \operatorname{Re} \left\{ \frac{\partial \varphi_{hes} \left(\frac{k\pi}{b-a}; u_0 \right)}{\partial u_0} e^{ik\pi \frac{x-a}{b-a}} \right\} V_k. \quad (34)$$

The Greeks formulae for the Lévy processes can be obtained similarly.

4 Error Analysis

In the derivation of the COS formula there are three steps that introduce errors: The truncation of the integration range in the risk-neutral valuation formula, the substitution of the density by its cosine series expansion on the truncated range, and the substitution of the series coefficients by the characteristic function approximation. Therefore, the overall error consists of three parts:

1. The integration range truncation error:

$$\epsilon_1 := v(t_0, x) - v_1(t_0, x) = \int_{\mathbb{R} \setminus [a, b]} v(T, y) f_{Y|X}(y|x) dy. \quad (35)$$

2. The series truncation error on $[a, b]$:

$$\epsilon_2 := v_1(t_0, x) - v_2(t_0, x) = e^{-r\Delta t} \sum_{k=N}^{+\infty} A_k(x) \cdot V_k, \quad (36)$$

where $A_k(x)$ and V_k are defined in (13) and (16), respectively.

3. The error related to approximating $A_k(x)$ by $F_k(x)$ in (18):

$$\begin{aligned} \epsilon_3 &:= v_2(t_0, x) - v_3(t_0, x) \\ &= e^{-r\Delta t} \frac{2}{b-a} \sum_{k=0}^{N-1} \operatorname{Re} \left\{ \int_{\mathbb{R} \setminus [a, b]} e^{ik\pi \frac{y-a}{b-a}} f_{Y|X}(y|x) dy \right\} V_k. \end{aligned} \quad (37)$$

We do not have to take any error in the coefficients V_k into account here as we have a closed form solution, at least for the plain vanilla options considered in this paper.

The key to bound the errors lies in the decay rate of the cosine series coefficients. The convergence rate of the Fourier-cosine series depends on the properties of the functions on the expansion interval. We first give the definitions classifying the rate of convergence of the series for different classes of functions, taken from [5].

Definition 4.1 (Algebraic Index of Convergence). *The algebraic index of convergence $n(\geq 0)$ is the largest number for which*

$$\lim_{k \rightarrow \infty} |A_k| k^n < \infty, \quad k \gg 1,$$

where the A_k are the coefficients of the series. An alternative definition: If the coefficients of a series, A_k , decay asymptotically as

$$A_k \sim O(1/k^n), \quad k \gg 1,$$

then n is the algebraic index of convergence.

Definition 4.2 (Exponential Index of Convergence). *If the algebraic index of convergence $n(\geq 0)$ is unbounded – in other words, if the coefficients, A_k , decrease faster than $1/k^n$ for any finite n – the series is said to have exponential convergence. Alternatively, if*

$$A_k \sim O(\exp(-\gamma k^r)), \quad k \gg 1,$$

with γ , the ‘asymptotic rate of convergence’, constant, for some $r > 0$, then the series shows exponential convergence. The exponent r is the index of convergence.

For $r < 1$, the convergence is called subgeometric.

For $r = 1$, the convergence is either called supergeometric with

$$A_k \sim O(k^{-n} \exp(-(k/j) \ln(k))),$$

(for some $j > 0$), or geometric with

$$A_k \sim O(k^{-n} \exp(-\gamma k)). \tag{38}$$

The density of the GBM process is a typical function that has a geometrically converging cosine series expansion.

Proposition 4.1 (Convergence of Fourier-cosine series [5] p.70-71). *If $g(x) \in \mathbb{C}^\infty([a, b] \subset \mathbb{R})$, then its Fourier-cosine series expansion on $[a, b]$ has geometric convergence. The constant γ in (38) is determined by the location in the complex plane of the singularities nearest to the expansion interval. Exponent n is determined by the type and strength of the singularity.*

If a function $g(x)$, or any of its derivatives, is discontinuous, its Fourier-cosine series coefficients show algebraic convergence. Integration-by-parts shows that the algebraic index of convergence, n , is at least as large as n' , with the n' -th derivative of $g(x)$ integrable.

References to the proof of this proposition are available in [5].

The following proposition further bounds the series truncation error of an algebraically converging series:

Proposition 4.2 (Series truncation error of algebraically converging series [4]). *It can be shown that the series truncation error of an algebraically converging series behaves like:*

$$\sum_{k=N+1}^{\infty} \frac{1}{k^n} \sim \frac{1}{(n-1)N^{n-1}}$$

The proof can be found in [4], a standard textbook.

With the two propositions above, we can state the following lemmas:

Lemma 4.1. *Error ϵ_3 merely consists of integration range truncation errors, and can be bounded by:*

$$|\epsilon_3| < |\epsilon_1| + Q |\epsilon_4|, \quad (39)$$

where Q is some constant independent of N and

$$\epsilon_4 := \int_{\mathbb{R} \setminus [a,b]} f_{Y|X}(y|x) dy.$$

Proof. Assuming that $f_{Y|X}$ is a real function, we rewrite (37) as

$$\epsilon_3 = e^{-r\Delta t} \frac{2}{b-a} \sum_{k=0}^{N-1} V_k \int_{\mathbb{R} \setminus [a,b]} \cos\left(k\pi \frac{y-a}{b-a}\right) f_{Y|X}(y|x) dy.$$

After interchanging the summation and integration, we rewrite $\sum_{k=0}^{N-1}$ as $(\sum_{k=0}^{+\infty} - \sum_{k=N}^{+\infty})$ and replace the cosine expansion of $v(T, y)$ in y by $v(T, y)$ itself:

$$\begin{aligned} \epsilon_3 &= e^{-r\Delta t} \int_{\mathbb{R} \setminus [a,b]} \left[v(T, y) - \sum_{k=N}^{+\infty} \cos\left(k\pi \frac{y-a}{b-a}\right) \cdot \frac{2}{b-a} V_k \right] f_{Y|X}(y|x) dy \\ &= \epsilon_1 - e^{-r\Delta t} \frac{2}{b-a} \int_{\mathbb{R} \setminus [a,b]} \left[\sum_{k=N}^{+\infty} \cos\left(k\pi \frac{y-a}{b-a}\right) \cdot V_k \right] f_{Y|X}(y|x) dy. \end{aligned} \quad (40)$$

According to Propositions 4.1 and 4.2, the V_k show at least algebraic convergence and we can therefore bound the expression as follows,

$$\left| \sum_{k=N}^{+\infty} \cos\left(k\pi \frac{y-a}{b-a}\right) \cdot V_k \right| \leq \sum_{k=N}^{+\infty} |V_k| \leq \frac{Q^*}{(N-1)^{n-1}} \leq Q^*, \quad \text{for } N \gg 1, n \geq 1,$$

for some positive constant Q^* . It then follows from (40) that

$$|\epsilon_3| < |\epsilon_1| + Q |\epsilon_4|$$

with $Q := 2e^{-r\Delta t} Q^* / (b-a)$ and $\epsilon_4 := \int_{\mathbb{R} \setminus [a,b]} f_{Y|X}(y|x) dy$, which depends on the size of $[a, b]$. \square

So, two out of the three error components are truncation range related. When the truncation range is sufficiently large, the overall error is dominated by ϵ_2 .

Equation (36) indicates that ϵ_2 depends on both $A_k(x)$ and V_k , the series coefficients of the density and that of the payoff, respectively. We assume that the density is typically more smooth than the payoff functions in finance and that the coefficients A_k decay faster

than V_k . Consequently, the product of A_k and V_k converges faster than either one of them, and we can bound this product as follows,

$$\left| \sum_{k=N}^{+\infty} A_k(x) \cdot V_k \right| \leq \sum_{k=N}^{+\infty} |A_k(x)|. \quad (41)$$

Error ϵ_2 is thus dominated by the series truncation error of the density function.

Proposition 4.3 (Series truncation error of geometrically converging series [5] p.48). *If a series has geometrical convergence, then the error after truncation of the expansion after $(N + 1)$ terms, $E_T(N)$, reads*

$$E_T(N) \sim P^* \cdot \exp(-N\nu).$$

Here, constant $\nu > 0$ is called the asymptotic rate of convergence of the series, which satisfies,

$$\nu = \lim_{n \rightarrow \infty} (-\log |E_T(n)|/n),$$

and P^* denotes a factor which varies less than exponentially with N .

Lemma 4.2. *Error ϵ_2 converges exponentially in the case of density functions $\in \mathbb{C}^\infty([a, b])$.*

$$|\epsilon_2| < P \cdot \exp(-(N - 1)\nu), \quad (42)$$

where $\nu > 0$ is a constant and P is a term that varies less than exponentially with N .

The proof of this is straightforward, applying Theorem 4.3 to (41).

Based on Proposition 4.2, we can prove the following lemma.

Lemma 4.3. *Error ϵ_2 can be bounded for densities having discontinuous derivatives, as follows:*

$$|\epsilon_2| < \frac{\bar{P}}{(N - 1)^{\beta-1}}, \quad (43)$$

where \bar{P} is a constant and $\beta \geq n \geq 1$ (n the algebraic index of convergence of V_k).

The proof of this lemma is straightforward. Note that $\beta \geq n$ is because the density function is usually more smooth than a payoff function.

Collecting the results (35), (39), (42) and (43), we can summarize that, with a properly chosen truncation of the integration range, the overall error converges either exponentially for density functions that belong to \mathbb{C}^∞ , i.e.

$$|\epsilon| < 2|\epsilon_1| + Q|\epsilon_4| + Pe^{-(N-1)\nu}, \quad (44)$$

or algebraically for density functions with discontinuous derivatives, i.e.

$$|\epsilon| < 2|\epsilon_1| + Q|\epsilon_4| + \frac{\bar{P}}{(N - 1)^{\beta-1}}. \quad (45)$$

To determine the size of the truncation range as a multiple of the standard deviation of $\ln(S_T/K)$, we use a rule of thumb, from [18]:

$$b - a = L \cdot \sqrt{-\frac{\partial^2 \phi(T, \omega)}{\partial \omega^2} \Big|_{\omega=0} + \left(\frac{\partial \phi(T, \omega)}{\partial \omega} \Big|_{\omega=0} \right)^2} \quad (46)$$

where $\phi(t, \omega)$ is the characteristic function of $\ln(S_t/K)$ conditional upon $\ln(S_0/K)$, and L is a proportionality constant, which can be chosen as $L = 10$ for smooth Gaussian density functions but should be chosen somewhat larger in the case of fat tails. The center of the expansion interval is placed at $\ln(S_0/K)$.

5 Numerical Results

In this section, we will perform a variety of numerical tests to evaluate the efficiency and accuracy of the COS method. We first focus on the plain vanilla European options and consider different processes for the underlying from geometric Brownian motion to the the Heston stochastic volatility process and the infinite activity Lévy processes Variance Gamma and CGMY. in the latter case we choose a value for parameter Y close to 2, representing a distribution with very heavy tails. We will choose long and short maturities in the tests, and as a final example we will also consider a digital option.

The underlying density functions for each individual experiment are also recovered with the help of the cosine series based inverse technique presented in Section 2. This may help the reader to get some insight in the relationship between the error convergence and the properties of the densities.

We compare our results with the COS method to two of its competitors for European option pricing, the Carr-Madan method [7] and the CONV method [17]. However, contrary to the common implementations of these methods we use the Simpson's rule for the Fourier integrals in order to achieve fourth order convergent techniques. Also in that case the FFT can be used for the Carr-Madan as well as for the CONV method. In all experiments, we set the same truncation range of the density domain for the COS and the CONV method. By these numerical experiments and comparisons with the other methods, we aim to demonstrate the stability and robustness of the new COS method, also under extreme conditions.

It should be noticed that parameter N in the experiments to follow denotes, for the COS method, the number of terms in the Fourier cosine expansion, and the number of grid points for the other two methods.

All CPU times presented, in milliseconds, are determined after averaging the computing times obtained from 100 experiments. The computer used for all experiments in this paper has an Intel(R) Pentium(R) 4 CPU, 2.80GHz with cache size 1024 KB; The code is written in Matlab 7-4.

5.1 Geometric Brownian Motion, GBM

The first set of experiments are performed under the GBM process with a short time to maturity. Parameters chosen for this test are:

$$S_0 = 100, r = 0.1, q = 0, T = 0.1, \sigma = 0.25. \quad (47)$$

Domain length parameter in (46) $L = 10$.

The convergence behavior at three different strike prices, $K = 80, 100$ and 120 , is checked. Reference values for these tests are based on an accurate adaptive integration scheme with a large number of points, of the Carr-Madan formula.

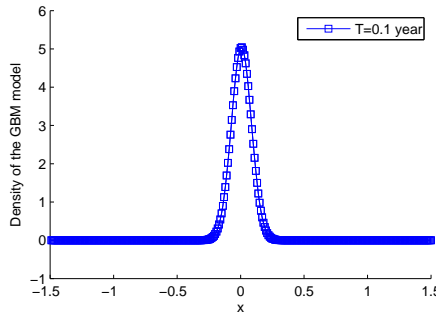


Figure 1: Recovered density function of the GBM model involved in the experiments; $K = 100$, other parameters as in (47).

Figure 1 shows that the recovered density function with small maturity time T has narrow tails. This implies that the tails of the characteristic function in the Fourier domain are fat. As a result, the truncation range for the Carr-Madan method in the Fourier domain has to be chosen relatively large. Therefore, a significantly larger value of N is necessary, compared to the other two methods to achieve the same level of accuracy.

Remark 5.1. *It is known that some experience is helpful for choosing the correct truncation range and damping factor α in Carr-Madan's method. A suitable choice appears to be damping $\alpha = 0.75$, which is also chosen in the experiments in this section.*

The CONV method can be used without any form of damping for most common option parameters.

As shown in Figure 2, the error convergence of the COS method is exponential (geometric) and superior to that of the 4-th order CONV and Carr-Madan methods. Already with $N = 2^7$, the COS results coincide with the reference values that are 12 to 13 digits accurate. Further, we observe that the error convergence rate is basically the same for the different strike prices. Notice that the results for these strikes, for certain N , can be obtained in one single numerical test with the COS method.

In Table 2, cpu time and error convergence information is displayed for the case $K = 100$, comparing the COS and the CONV methods. To get the same level of accuracy, the

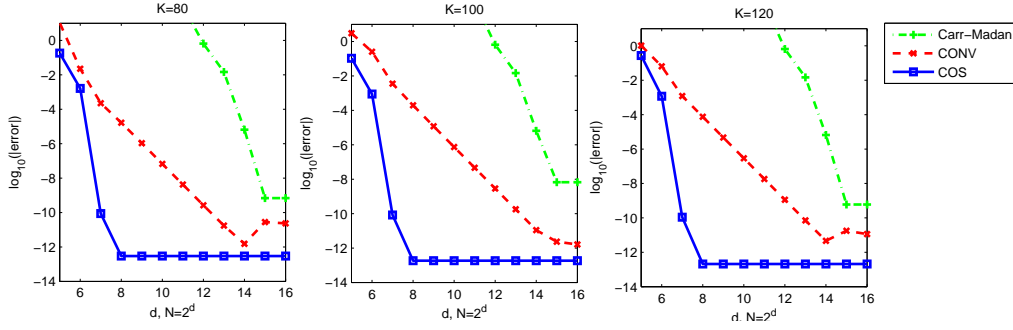


Figure 2: COS vs. CONV in error convergence for pricing European call options under GBM model

COS method uses significantly fewer cpu time; This becomes more prominent when the desired accuracy is high.

Remark 5.2. *We have observed a linear computational complexity for the COS method by doubling N and performing the computations. In Table 2 this cannot be observed as the biggest portion of time spent in the experiments with relatively small N is computational overhead.*

Table 2: Error convergence and cpu time comparing the COS and CONV methods for European options under GBM, parameters as in (47), $K = 100$. Reference $v(0, 100) = 3.65996845\dots$

	(N)	32	64	128	256	512
COS	msec	0.0441	0.0418	0.0607	0.1006	0.1940
	error	1.06e-01	8.87e-04	8.31e-11	1.85e-13	1.85e-13
CONV	msec	0.0388	0.0403	0.0464	0.0651	0.1147
	error	3.0275	2.56e-01	3.57e-03	1.97e-04	1.20e-05

5.1.1 Cash-or-nothing Option

We confirm that the convergence of the COS method does not depend on a discontinuity in the payoff function, provided we have an analytic expression for the coefficients V_k by pricing a cash-or-nothing call option here. The underlying process is GBM, so that an analytic solution exists. Parameters chosen for this test are:

$$S_0 = 100, K = 120, r = 0.05, q = 0, T = 0.1, \sigma = 0.2, L = 10. \quad (48)$$

Table 3 presents the exponential convergence of the COS method.

Table 3: Error and cpu time for a cash-or-nothing call option with the COS method, parameters as in (48); Reference $v(0, 90) = 0.27330649649\dots$

N	40	60	80	100	120	140
error	2.46e-02	1.64e-02	6.35e-04	6.85e-06	2.44e-08	2.79e-11
cpu time (sec.)	0.0330	0.0334	0.0376	0.0428	0.0486	0.0497

5.2 Heston's Model

As a second test we choose the Heston model with the following parameters:

$$\begin{aligned} S_0 &= 100, K = 100, r = 0, q = 0, \lambda = 1.5768, \eta = 0.5751, \\ \bar{u} &= 0.0398, u_0 = 0.0175, \rho = -0.5711. \end{aligned} \quad (49)$$

Two maturity dates are chosen and the length of the domain L is set accordingly. We evaluate $T = 1$ with $L = 10$ and $T = 10$ with $L = 30$.

In (46) we need to compute the standard deviation of the Heston model, which is not trivial. The standard deviation can, however, be approximated well by the quantity $\sqrt{\bar{u} + \bar{u}\eta}$, which is done for this experiment. Figure 3 presents the recovered density

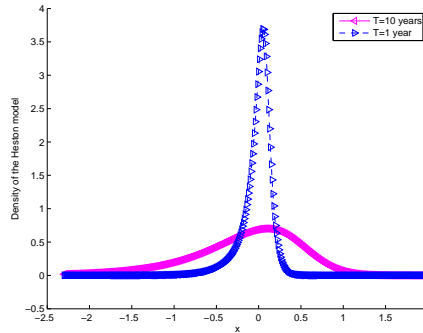


Figure 3: Recovered density functions of the Heston experiments, parameters as in (49).

functions. It shows that $T = 10$ gives rise to somewhat fatter tails in the density function.

In this test we compare the COS method with the Carr-Madan method, which is state-of-the-art for the calibration of Heston model in industry. The truncated Fourier domain for the Carr-Madan method is set to $[0, 1000]$ for the experiment with $T = 1$, and to $[0, 500]$ for $T = 10$. The option price reference values are obtained by the Carr-Madan method using $N = 2^{18}$ points. We find $v(0, S_0) = 5.785155435\dots$ for $T = 1$ and $v(0, S_0) = 22.318945791474590$ for $T = 10$.

Tables 4 and 5 illustrate the high efficiency of the COS method as compared to the Carr-Madan method.

Table 4: Error convergence and cpu times for the COS and Carr-Madan methods for Heston’s model with $T = 1$, parameters as in (49).

COS			Carr-Madan		
N	error	time (msec.)	N	error	time (msec.)
40	4.69e-02	0.0607	512	1.79e+06	0.6702
80	3.81e-04	0.0805	1024	2.16e+01	1.1874
120	1.17e-05	0.1078	2048	2.61e-01	1.9373
160	6.18e-07	0.1300	4096	2.15e-03	3.5577
200	3.70e-09	0.1539	8192	1.40e-07	7.5376

Table 5: Error convergence and cpu time for the COS and Carr-Madan methods for Heston’s model with $T = 10$, parameters as in (49).

COS			Carr-Madan		
N	error	time (msec.)	N	error	time (msec.)
40	4.96e-01	0.0598	512	3.27e+01	1.2260
65	4.63e-03	0.0747	1024	2.61e-01	1.1872
90	1.35e-05	0.0916	2048	2.15e-03	2.0237
115	1.08e-07	0.1038	4096	1.11e-07	3.8807
140	9.88e-10	0.1230	8192	2.70e-08	7.5381

Note that all computations are really fast as the times are given in milli-seconds. The COS method, however, appears to be approximately a factor 20 faster than the Carr-Madan method. As an example of its efficiency we observe from the tables that for $N < 200$ the COS method gives results that are accurate up to the 7th digit within 0.15 milliseconds.

The convergence rate of the COS method is somewhat slower for the short maturity example, as compared to the 10 years maturity. This is due to the fact that the density function for the latter case is more smooth, as seen in Figure 3. When a density function belongs to the class of \mathbb{C}^∞ functions, the Fourier cosine series has an exponentially convergence behaviour. The COS convergence rate for small T is, however, still exponential in Heston’s model.

5.3 Variance Gamma, VG

As a next example we price options under the Variance Gamma process, which is from the class of infinite activity Lévy processes. The VG process is usually parameterised with parameters σ, θ and ν related to C, G and M in (28) through:

$$C = \frac{1}{\nu}, \quad G = \frac{\theta}{\sigma^2} + \sqrt{\frac{\theta^2}{\sigma^4} + \frac{2}{\nu\sigma^2}}, \quad M = -\frac{\theta}{\sigma^2} + \sqrt{\frac{\theta^2}{\sigma^4} + \frac{2}{\nu\sigma^2}}, \quad (50)$$

The parameters chosen in the numerical experiments are:

$$K = 90, S_0 = 100, r = 0.1, q = 0, \sigma = 0.12, \theta = -0.14, \nu = 0.2. \quad (51)$$

This case has been chosen because a relatively slow convergence was reported for the CONV method for very short maturities in [17]. Here, we compare the convergence for $T = 1$ (with $L = 10$) and for $T = 0.1$ year (setting $L = 20$).

Figure 4 presents the difference in shape of the two recovered density functions. For $T = 0.1$, the density is much more peaked. Notice that for $T = 0.1$ the error convergence

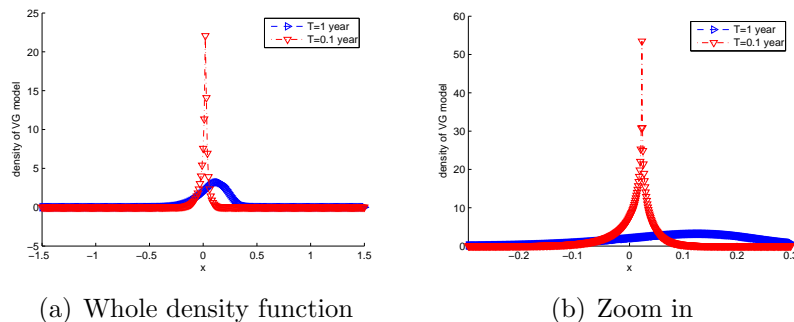


Figure 4: Recovered density functions for the VG model and two maturity dates; $K = 90$, other parameters as in (51).

Table 6: Convergence of the COS method for the VG model with $K = 90$, parameters as in (51).

$T = 0.1$; Reference $v(0, 90) = 19.09935472\dots$			$T = 1$; Reference $v(0, 90) = 10.993703186\dots$		
N	error	time(msec.)	N	error	time(msec.)
128	5.43e-04	0.0709	30	6.08e-04	0.0379
256	7.08e-05	0.1178	60	1.89e-07	0.0473
512	3.80e-06	0.2130	90	1.60e-08	0.0592
1024	2.35e-05	0.1049	120	5.97e-10	0.0731
2048	1.41e-07	0.7809	150	3.29e-12	0.0811

of the COS method is algebraic instead of exponential, so that the convergence is slower in this case. This is in agreement with the recovered density function in Figure 4, which is clearly not in C^∞ . In the extreme case, we would observe a delta function alike curve for $T \rightarrow 0$. According to the error analysis, in the presence of discontinuities in the derivatives, the error convergence rate of the COS method degrades from exponential to algebraic.

We also plot the errors in Figure 5, comparing the convergence of the COS method to that of the (N^{-2}) -CONV method⁴. The convergence rate of the COS method for $T = 1$ is significantly faster than that of the CONV method, but for $T = 0.1$ the convergence is comparable.

⁴The Simpson rule did not improve the convergence rate here.

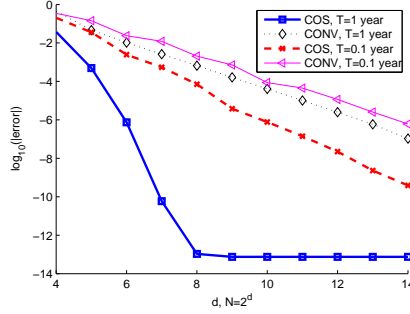


Figure 5: Convergence of the COS method for VG model

5.4 CGMY Process

Finally, we evaluate the method's convergence for the CGMY model. It has been reported in [1, 21] that PIDE methods have difficulty solving the cases for which $1 \leq Y \leq 2$. Therefore we evaluated the COS method with $Y = 0.5$, $Y = 1.5$ and $Y = 1.98$, respectively. The other parameters are chosen as follows:

$$S_0 = 100, K = 100, r = 0.1, q = 0, C = 1, G = 5, M = 5, L = 10, T = 1. \quad (52)$$

In Figure 6, the recovered density functions for the three cases are plotted. For large values

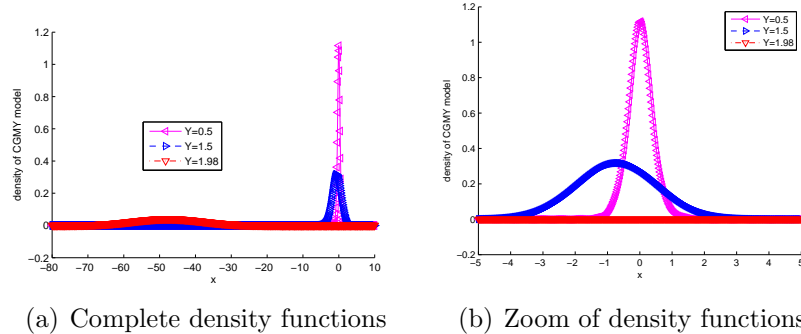


Figure 6: Recovered density functions for the CGMY model with different values of Y ; other parameters as in (52).

of Y the tails of the density function are fatter and the center of the distribution shifts.

Therefore, we used adapted truncation ranges in this case: $[-L \cdot Y, L \cdot Y]$ for $Y = 0.5$ and $Y = 1.5$ with $L = 10$ and the range is set to $[-100, 20]$ for $Y = 1.98$; Reference values for the numerical experiments are computed with the COS method with $N = 2^{19}$, as there are no reference values available for the latter cases. The numerical results are presented in Tables 7 and 8, for $Y = 0.5$ and $Y = 1.5$, respectively.

Again, the COS method converges exponentially, which is faster than the 4th order convergence of the CONV method With a relatively small values of N , i.e. $N \leq 100$,

Table 7: Comparison of the COS and CONV methods in accuracy and speed for CGMY with $Y = 0.5$ and the other parameters from (52); Ref.val.=19.8129487706...

COS			CONV		
N	error	time (msec.)	N	error	time (msec.)
40	3.82e-02	0.0560	64	2.13e-02	0.0595
60	6.87e-04	0.0645	128	6.42e-04	0.0836
80	2.11e-05	0.0844	256	3.82e-05	0.1366
100	9.45e-07	0.1280	512	2.30e-06	0.2551
120	5.56e-08	0.1051	1024	9.86e-08	0.4957
140	4.04e-09	0.1216	2048	2.93e-08	0.9893

Table 8: Comparison of the COS and CONV methods in accuracy and speed for CGMY with $Y = 1.5$ and the other parameters from (52); Ref.val.=49.790905305...

COS			CONV		
N	error	time (msec.)	N	error	time (msec.)
40	1.38e+00	0.0545	64	1.17e-02	0.0600
45	1.98e-02	0.0589	128	6.92e-04	0.0928
50	4.52e-04	0.0689	256	4.26e-05	0.1622
55	9.59e-06	0.0690	512	2.73e-06	0.2776
60	1.22e-09	0.0732	1024	3.93e-07	0.5189
65	7.53e-10	0.0748	2048	2.18e-07	0.9773

the COS results are accurate up to 7 digits. The computational time spent is less than 0.1 millisecond. Comparing Tables 7 and 8, we notice that the convergence rate with $Y = 1.5$ is faster than that of $Y = 0.5$, as opposed to the convergence of the CONV method. Density functions from fat-tailed distributions can often be represented well by cosine basis functions.

Table 9: The COS method for CGMY model with $Y = 1.98$; other parameters as in (52). Reference value = 0.252104475...

N	20	25	30	35	40
msec	0.0438	0.0463	0.0485	0.0511	0.0538
error	4.17e+02	5.15e-01	6.54e-05	1.10e-09	1.94e-15

6 Conclusions and Discussion

In this paper we introduced an option pricing method based on Fourier-cosine series expansions, the COS method, for pricing European options. The method can be used as long as a characteristic function for the underlying price process is available. It is accompanied by an error analysis. In several numerical experiments, the convergence rate of the COS method is exponential in accordance with the analysis. However, when the density function of the underlying process has a discontinuity in its derivatives an algebraic convergence is expected and observed. Especially for European options the series coefficients of the payoff functions can be obtained analytically. The computational complexity of the COS method is linear in N , the number of terms chosen in the Fourier-cosine series expansion. Very fast computing times are reported here for the Heston and Lévy models. With $N < 150$ all numerical results obtained were accurate up to 8 digits, in less than 0.5 milliseconds of cpu time.

The generalization to high dimensional option pricing problems, however, is not trivial, because an analytic formula for the coefficients V_k cannot easily be obtained. The V_k should then be recovered numerically, which has an impact on the convergence rate of the COS method.

References

- [1] ALMENDRAL A., AND OOSTERLEE C.W., Accurate Evaluation of European and American Options Under the CGMY Process., *SIAM J. Sci. Comput.* 29: 93-117, 2007.
- [2] ANDRICOPOULOS A.D., WIDDICKS M., DUCK P.W. AND NEWTON D.P., Universal option valuation using quadrature methods, *J. Fin. Economics*, 67: 447-471, 2003.
- [3] ANDRICOPOULOS A.D., WIDDICKS M., DUCK P.W. AND NEWTON D.P., Extending quadrature methods to value multi-asset and complex path dependent options, *J. Fin. Economics*, 2006.
- [4] BENDER C.M. AND ORSZAG S.A., *Advanced Mathematical Methods for Scientists and Engineers*. McGraw-Hill, New York, 1978.
- [5] BOYD J.P., *Chebyshev & Fourier Spectral Methods*, Springer-Verlag, Berlin, 1989.
- [6] CARR P.P., GEMAN H., MADAN D.B. AND YOR M., The fine structure of asset returns: An empirical investigation. *J. of Business*, 75: 305-332, 2002.
- [7] CARR P.P. AND MADAN D.B., Option Valuation Using the Fast Fourier Transform. *J. Comp. Finance*, 2:61-73, 1999.

- [8] CHOURDAKIS K., Option pricing using the Fractional FFT. *J. Comp. Finance* 8(2), 2004.
- [9] CONT R. AND TANKOV P., *Financial modelling with jump processes*, Chapman and Hall, Boca Raton, FL, 2004.
- [10] D. DUFFIE, J. PAN AND K. SINGLETON, *Transform analysis and asset pricing for affine jump-diffusions*. *Econometrica* 68: 1343–1376, 2000.
- [11] D. DUFFIE, D. FILIPOVIC AND W. SCHACHERMAYER, Affine Processes and Applications in Finance. *Ann. of Appl. Probab.*, 13(3): 984-1053, 2003.
- [12] EVANS G.A. AND WEBSTER J.R., A comparison of some methods for the evaluation of highly oscillatory integrals. *J. of Comp. Applied Math.* 112: 55-69, 1999.
- [13] E.G. HAUG, *The complete guide to option pricing formulas*. McGraw-Hill, 1998.
- [14] HESTON S., A closed-form solution for options with stochastic volatility with applications to bond and currency options. *Rev. Financ. Studies*, 6: 327-343, 1993.
- [15] HULL J.C. *Options, futures and other derivatives* Prentice Hall. 4th ed., 2000.
- [16] LEWIS A. *A simple option formula for general jump-diffusion and other exponential Lévy processes*. SSRN working paper, 2001. Available at: <http://ssrn.com/abstract=282110>.
- [17] LORD R., FANG F., BERVOETS F. AND OOSTERLEE C.W., *A Fast and Accurate FFT-Based Method for Pricing Early-Exercise Options under Lévy Processes*. SSRN, page <http://ssrn.com/abstract=966046>, 2007. To appear in SIAM J. Sci. Comput.
- [18] O’SULLIVAN C., *Path Dependent Option Pricing under Lévy Processes* EFA 2005 Moscow Meetings Paper, Available at SSRN: <http://ssrn.com/abstract=673424>, Febr. 2005
- [19] PIESSENS R. AND POLEUNIS F., A Numerical Method for The Integration of Oscillatory Functions, *BIT*, 11: 317-327, 1971.
- [20] RAIBLE S., *Lévy Processes in Finance: Theory, Numerics and Empirical Facts* PhD Thesis, Inst. für Math. Stochastik, Albert-Ludwigs-Univ. Freiburg, 2000.
- [21] WANG I., WAN J.W. AND FORSYTH P., Robust numerical valuation of European and American options under the CGMY process. *J. Computational Finance*, 10(4): 31-70, 2007.

A Matlab Code for Lévy and Heston's Model

All input parameters are denoted by the same notations as given in the text, except for

- “q”: continuous dividend rate.
- “CP”: a flag that switches to call options when it equals 1 and to put options when it equals -1 .
- “Model”: a flag that switches among different underlying processes.
- “Params”: a vector that holds parameters for the specified underlying process.

```
function C = Euro_Cos(L, S0, CP, K, T, q, r, Model, Params, N)
    mu=r-q; qstar=L*gridvol_model(T,Model,Params); x0=log(S0/K);
    b=qstar;a=-qstar; j = [0:N-1]; co =pi/(b-a); omega = j*co;
%Series coefficients for the density
    cf=cf_model(omega, mu, dt, Model, Params);
    fj=real(cf.*exp(i*j*co*(x0-a)))*2/(b-a); fj(1)=0.5*fj(1);
%Series coefficients for the payoff
    if CP==1
        c=0;d=b;
    else
        c=a;d=0;
    end
    dma = (d-a)/(b-a)*pi;    cma= (c-a)/(b-a)*pi;
    expd=exp(d);    expc=exp(c);
    Chi = (cos(j*dma)*expd - cos(j*cma)*expc +...
        j*co.* (sin(j*dma)*expd - sin(j*cma)*expc) )./(1+(j*co).^2);
    Psi = (sin(j(2:end)*dma) - sin(j(2:end)*cma))./(co*j(2:end));
    Psi=[d-c, Psi];
    vj = CP*K*(Chi-Psi);
%Final pricing formula
    C = exp(-r*dt)*sum(fj.*vj);
return;
```

Note that two inner-called programs, `gridvol_model(dt,Model,Params)` and `cf_model(omega,mu,dt)` return the standard deviation and the characteristic function values of the specified underlying process, respectively.